

# Flexible Electrochromic Devices Based on Optoelectronically Active Polynorbornene Layer and Ultratransparent Graphene Electrodes

Wei-Ren Lian,<sup>†</sup> Ying-Chi Huang,<sup>†</sup> Yi-An Liao,<sup>‡</sup> Kun-Li Wang,<sup>§</sup> Lain-Jong Li,<sup>⊥</sup> Ching-Yuan Su,<sup>⊥</sup> Der-Jang Liaw,<sup>†,\*</sup> Kueir-Rarn Lee,<sup>||</sup> and Juin-Yih Lai<sup>||</sup>

<sup>†</sup>Department of Chemical Engineering, National Taiwan University of Science and Technology, 10607 Taipei, Taiwan

<sup>‡</sup>School of Medicine, Faculty of Medicine, National Yang-Ming University, Taipei, Taiwan

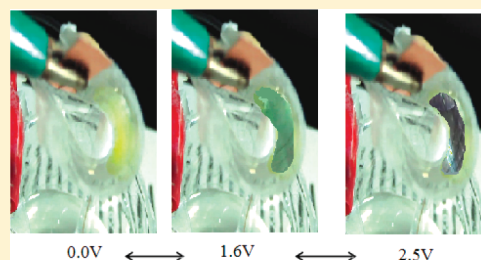
<sup>§</sup>Department of Chemical Engineering and Biotechnology, National Taipei University of Technology, 10608 Taipei, Taiwan

<sup>⊥</sup>Research Center for Applied Sciences, Academia Sinica, Taipei 11529, Taiwan

<sup>||</sup>R&D Center for Membrane Technology, Department of Chemical Engineering, Chung Yuan University, 32023 Chung-Li, Taiwan

**S** Supporting Information

**ABSTRACT:** Novel electrochromic polynorbornenes poly(NBPYTPAM) and poly(HNBPYTPAM), containing electroactive chromophores, were prepared via ring-opening metathesis polymerization (ROMP) from a new norbornene derivative (NBPYTPAM) using Grubbs' catalyst and followed by hydrogen reduction. The glass transition temperatures ( $T_g$ ) of poly(NBPYTPAM) and hydrogenated poly(HNBPYTPAM) were 190 and 175 °C, respectively. The cyclic voltammogram of the poly(HNBPYTPAM) film cast onto flexible graphene-coated polyethylene terephthalate (PET) substrates exhibited two reversible oxidation redox couples at 1.0 and 1.9 V. Flexible electrochromic devices were fabricated from the electroactive polymers and graphene-coated PET substrates. The electrochromic characteristics of poly(HNBPYTPAM) showed excellent stability and reversibility, with multistaged color changes from its yellow neutral form to green and then to dark-blue.



## 1. INTRODUCTION

Electrochromic materials typically comprise redox-active species which exhibit significant, lasting, and reversible changes in color upon the injection or withdrawal of electrons. Electrochromic devices attract great interest due to their potential use in various applications, such as information display and storage, automotive industry (rear-view mirrors), and smart windows in green architecture. Indium tin oxide (ITO) is widely used as the transparent electrodes for electrochromic devices; however, its increasing cost, mechanical brittleness, chemical instability and losses in conductivity on bending<sup>1</sup> retards its applications in flexible optoelectronics. The development of flexible electrochromic devices further extends their applications to the occasion requiring bendability such as for flexible electrochromic display and military camouflage. Monolayer graphene, a two-dimensional (2D) sheet of covalently bonded carbon atoms, has attracted great attention recently due to its high conductivity, good transmittance, excellent mechanical strength, high chemical stability and flexibility.<sup>2–7</sup> Graphene has been made by various methods such as mechanical exfoliation, ultrasonic cleavage of graphite, chemical oxidation of graphite, electrochemical exfoliation, epitaxial growth on silicon carbide and chemical vapor deposition (CVD).<sup>8–16</sup> Transparent conducting graphene electrodes have been used as electrodes in both dye-sensitized and polymer solar cells.<sup>17–20</sup> To the best of our knowledge, the combination of large-area, flexible and highly transparent CVD graphene electrodes with a highly

efficient electrochromic functional moiety triarylamine (TPA) have not been reported yet. Recent developments have shown that TPA possesses easy oxidizability and noticeable change in color.<sup>21–26</sup> Here we incorporate the TPA moiety with pyrenyl groups into a synthetic polynorbornene via ring-opening metathesis polymerization (ROMP) and followed hydrogenation to obtain saturated polynorbornene as the active and flexible electrochromic layer. The asymmetric structure with pyrenyl and triphenylamine groups in the norbornene derivative was designed to improve the thermal stability and solubility.<sup>26</sup> In addition, the 2,2-diphenyl propane structure in the polymer chain could enhance the chemical resistance.<sup>27</sup> The polynorbornene showed remarkable solvatochromism, excellent electrochemical stability and reversible electrochromic behavior. Electrochromic devices made from the thermally stable polynorbornene and high transparent graphene electrode coated on PET substrate (PHNBPYTPAM-G) was successfully fabricated.

## 2. RESULTS AND DISCUSSION

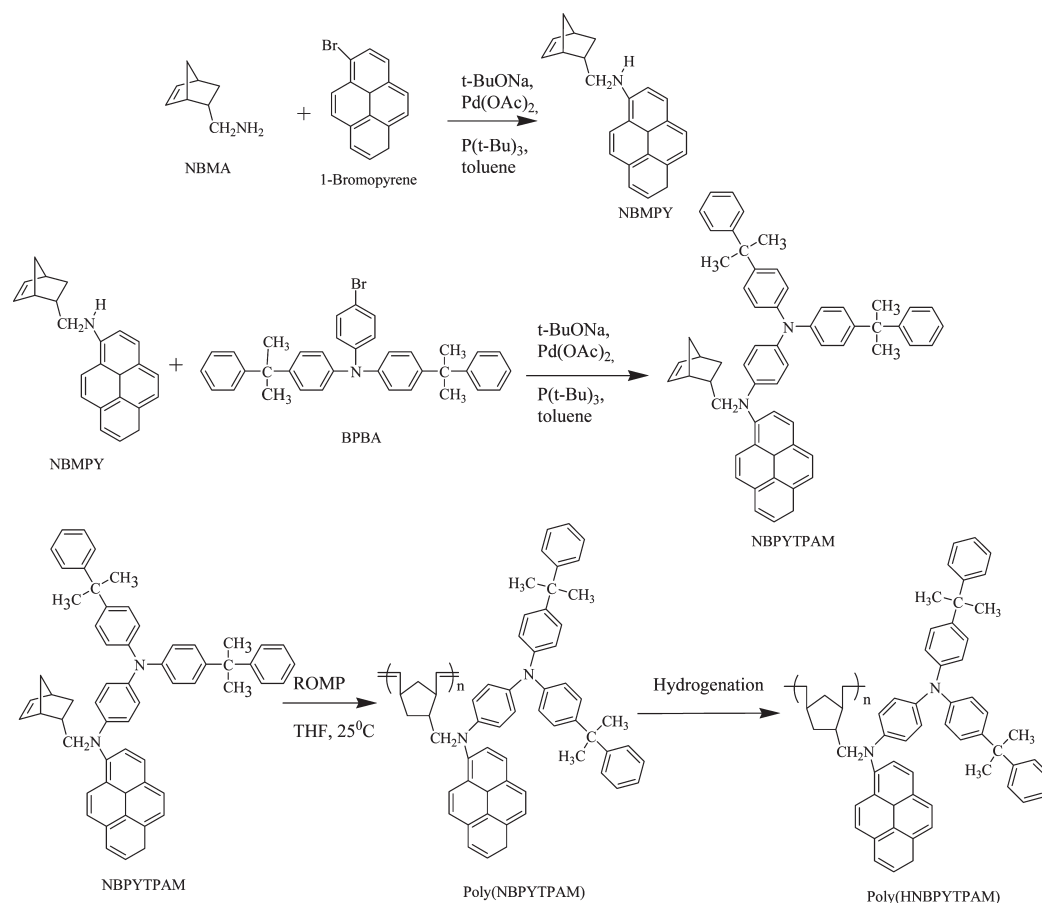
**2.1. Synthesis and Characterization.** The synthesis procedures of the norbornene monomer (NBPYTPAM) containing

**Received:** July 23, 2011

**Revised:** October 16, 2011

**Published:** November 29, 2011

Scheme 1. Preparation of Polynorbornenes Poly(NBPYTPAM) and Poly(HNBPYTPAM)



asymmetrical pyrenyl and triphenylamine substituents are outlined in Scheme 1. The norbornene derivative (NBPYTPAM) is successfully synthesized by the *N*-(4-bromophenyl)-4-(2-phenylpropan-2-yl)-*N*-(4-(2-phenylpropan-2-yl)phenyl)benzeneamine (BPBA) and 5-(pyrenylamino-methyl)-bicyclo[2.2.1]-hept-2-ene (NBMPY). Elemental analysis,  $^1\text{H}$  and  $^{13}\text{C}$  NMR as well as two-dimensional NMR techniques were used to identify structures of the norbornene derivative (NBPYTPAM). ( $^1\text{H}$  NMR shown in Figure S1, Supporting Information) The ratio of NBPYTPAM endo- and exo isomers is calculated to be 6:1 from NMR spectrum. Elemental analysis and NMR spectra clearly confirm that the compound, NBPYTPAM, is consistent with the proposed structures. The polynorbornene, poly(NBPYTPAM) ( $^1\text{H}$  NMR shown in Figure S2, Supporting Information) synthesized by ROMP using Ru (G3) with [monomer]/[catalyst] ( $[M]/[I] = 1500$ ) is shown in Scheme 1 and the molecular weight determined by gel permeation chromatography (GPC) was  $3.92 \times 10^5$  with yield of 92%. Because of the oxidation of unsaturated C=C double bonds in polynorbornenes will make poly(HNBPYTPAM) ( $^1\text{H}$  and  $^{13}\text{C}$  NMR shown in Figure S3, Supporting Information) unstable under air atmosphere, hydrogenation reaction of the unsaturated polynorbornene to get hydrogenated poly(HNBPYTPAM) had advantages in industrial application.<sup>28</sup> Poly(NBPYTPAM) was reduced using hydrogenating agent as shown in Scheme 1 to afford stable poly(HNBPYTPAM).

**2.1. Basic Properties.** Poly(HNBPYTPAM) is highly soluble in common organic solvents such as toluene, benzene, THF, dichloromethane, *p*-xylene and 1,2-dichlorobenzene. The excellent solubility makes the hydrogenated ring-opened polynorbornene poly(HNBPYTPAM) become a potential candidate for practical applications of spin-coating, dip-coating, or inject-printing processes to obtain the thin film for optoelectronic devices. In Figure 1A, there is no UV-vis absorption bands for monomer NBMA from 250 to 350 nm (curve e), and the absorption spectrum of monomer NBMPY containing the pyrene substituent showed two characteristic peaks at 285 and 400 nm (curve c). TPA exhibited strong absorption at 322 nm in THF solution (curve d). It means that the UV-vis absorption at 322 nm of poly(HNBPYTPAM) is assignable to a  $\pi-\pi^*$  transition resulting from the conjugated triphenylamine structure<sup>21,22,25</sup> and it is not related to cyclic norbornene and pyrene structure (curve a). The UV-vis absorption of poly(HNBPYTPAM) in solid state also shows similar absorbance peaks with a little red-shift at 323 nm (curve b). The PL spectrum of poly(HNBPYTPAM) in solid state showed the maximum band at 560 nm. Figure 1B showed the normalized PL spectra of poly(HNBPYTPAM) in various solvents, together with fluorescence images of the solutions. The PL emission spectra of poly(HNBPYTPAM) showed strong solvent-polarity dependence, and underwent remarkable bathochromic shifts with an increase of the solvent polarity. The fluorescent quantum yield for the poly(HNBPYTPAM) was 82.4% and

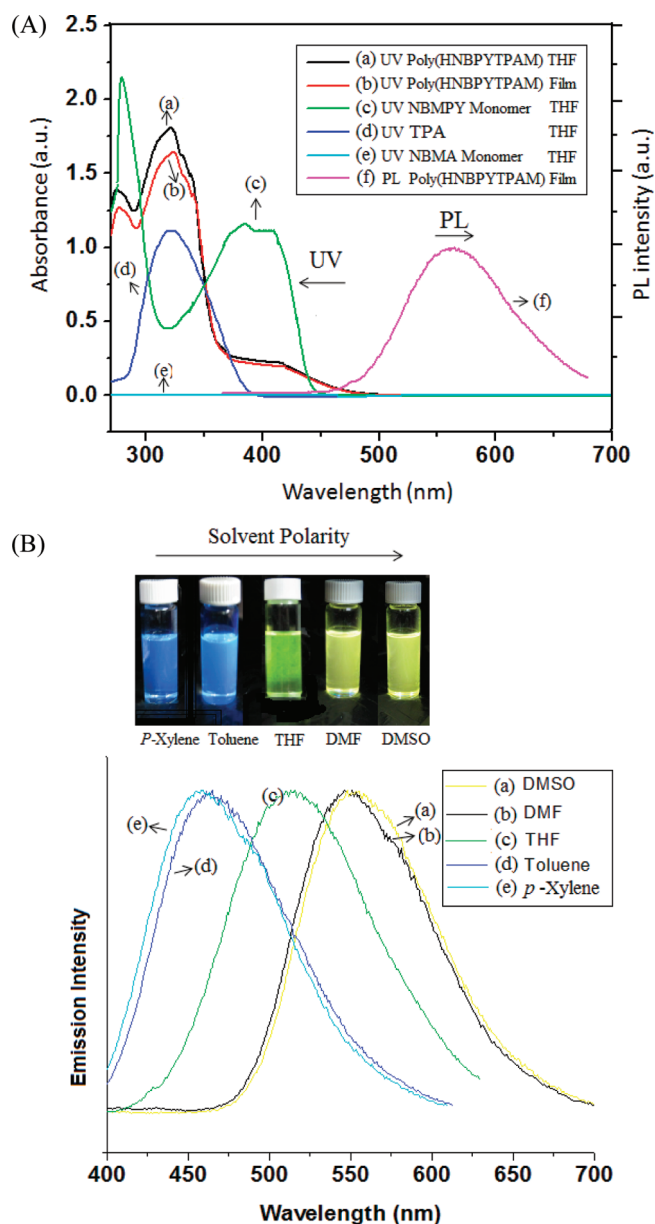


**Figure 1.** (A) UV-vis spectra of (a) poly(HNBPYTPAM) ( $1 \times 10^{-5}$  mol L $^{-1}$ ; THF), (b) poly(HNBPYTPAM) film, (c) NBMPY ( $1 \times 10^{-5}$  mol L $^{-1}$ ; THF), (d) TPA ( $1 \times 10^{-5}$  mol L $^{-1}$ ; THF), (e) NBMA ( $1 \times 10^{-5}$  mol L $^{-1}$ ; THF) and emission spectra of (f) poly(HNBPYTPAM) ( $1 \times 10^{-5}$  mol L $^{-1}$ ;  $\lambda_{\text{exc}} = 320$  nm; film). (B) Normalized PL spectra of dilute solutions of poly(HNBPYTPAM) ( $1 \times 10^{-3}$  mol L $^{-1}$ ) in solvents of various polarity. Photographs were taken under illumination of 365 nm UV light.

77.5% in THF solution and film, respectively. The emission color changed from blue in *p*-xylene to yellow in dimethyl sulfoxide (DMSO). The solvatochromism could be attributed to the fast intramolecular charge-transfer process resulting in a large change of dipole moment in the excited state.<sup>29</sup> The onset wavelength of poly(HNBPYTPAM) in solid state from the UV-vis transmittance spectrum is about 370 nm, by which the energy gap of poly(HNBPYTPAM) is estimated to be 3.3 eV.

**2.2. Thermal Properties.** The thermal properties of the conjugated polymers were investigated by DSC and TGA techniques.

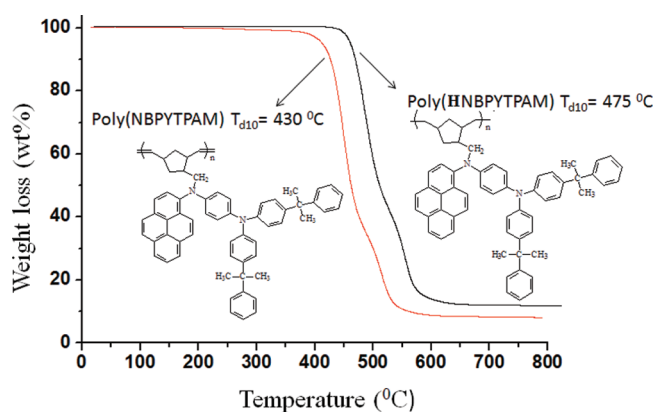


**Figure 2.** TGA curves for poly(NBEDPY) and hydrogenated poly(HNBEDPY) measured under nitrogen. Temperature was raised at a rate of 10 °C min $^{-1}$ .

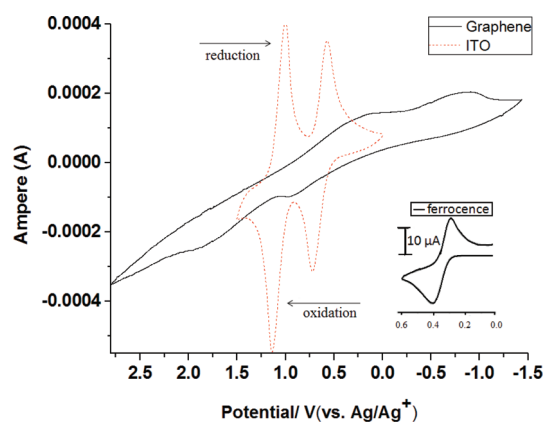


**Figure 3.** Cyclic voltammograms of poly(HNBPYTPAM) in films cast on graphene-coated PET substrate and ITO-coated glass substrate in CH $_3$ CN containing 0.1 M TBAP. The scanning rate is 0.1 V/s.

Poly(NBPYTPAM) and hydrogenated poly(HNBPYTPAM) both showed higher  $T_g$ s, respectively, at 186 and 136 °C than the reported polynorbornene (35 °C)<sup>30</sup> due to the incorporation of pendant aromatic triphenylamine and pyrene moieties. A decrease in  $T_g$  caused by the hydrogenation was about 50 °C due to the easier rotation around the hydrogenated carbon-carbon single bond. The unsaturated poly(NBPYTPAM) and hydrogenated poly(HNBPYTPAM) exhibited high 10% weight-loss temperatures ( $T_{d10}$ ), respectively, at 430 and 475 °C under nitrogen as shown in Figure 2 due to the asymmetric structure. The hydrogenated poly(HNBPYTPAM) was more stable than unsaturated poly(NBPYTPAM) with an increase in 10% decomposition temperature of about 45 °C under nitrogen.

**2.3. Electrochemical Properties.** The electrochemical behaviors of poly(HNBPYTPAM) were investigated by cyclic voltammetry (CV) conducted by films cast on graphene-coated polyethylene terephthalate (PET) substrates (named as PHNBPYTPAM-G electrodes here) and cast on ITO-coated glass substrates (named as PHNBPYTPAM-ITO electrodes here) as the working electrodes in dry CH $_3$ CN solution containing 0.1 M of TBAP as the electrolyte. The oxidative and reductive cycles of PHNBPYTPAM-G and PHNBPYTPAM-ITO are shown in Figure 3. PHNBPYTPAM-ITO performed different colors from light yellow to green, then to blue at applied potentials above 0.7 and



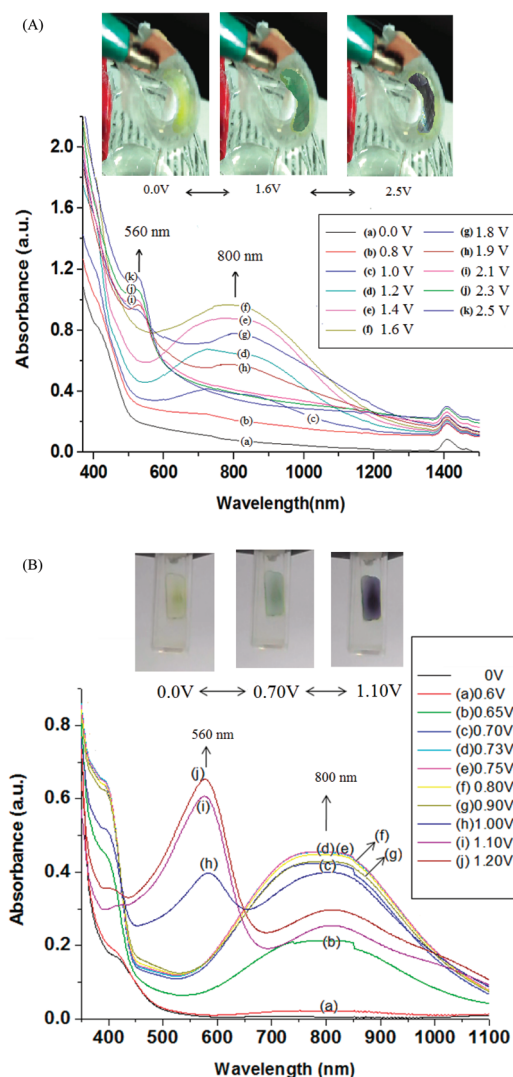


**Figure 4.** Absorption spectra of poly(HNBPYTPAM) in films cast on (A) flexible graphene-coated PET substrate (thickness approximately 10  $\mu\text{m}$ ) under  $E_{\text{appl}}$  0–2.5 V. (B). ITO-coated glass substrate (thickness approximately 11  $\mu\text{m}$ ) under  $E_{\text{appl}}$ : 0–1.2 V in  $\text{CH}_3\text{CN}$  with 0.1 M TBAP as the supporting electrolyte.

1.1 V in the oxidative scan, respectively. Because of the higher sheet resistance of graphene than that of ITO, the flexible PHNBPYTPAM-G just showed higher oxidation potentials than the inflexible PHNBPYTPAM-ITO, and PHNBPYTPAM-G performed color changes from light yellow to green, then to blue at applied potentials above 1.0 and 1.9 V in the oxidative scan, respectively. The CV of PHNBPYTPAM-G electrode showed weaker and broader redox waves than PHNBPYTPAM-ITO electrode. The potential separation between oxidation and reduction waves of PHNBPYTPAM-G electrode is also larger than that of PHNBPYTPAM-ITO electrode. This is possibly due to that the high resistance of graphene electrode changed the potential of working electrode, which made the oxidation wave of PHNBPYTPAM more positive and the corresponding reduction wave more negative. The electrochromic characteristics will be discussed below.

The CV of the polymer was examined with 100 cycles as shown in the Supporting Information [see Figure S4]. The currents decayed as the repeated scanning, but the redox potentials were

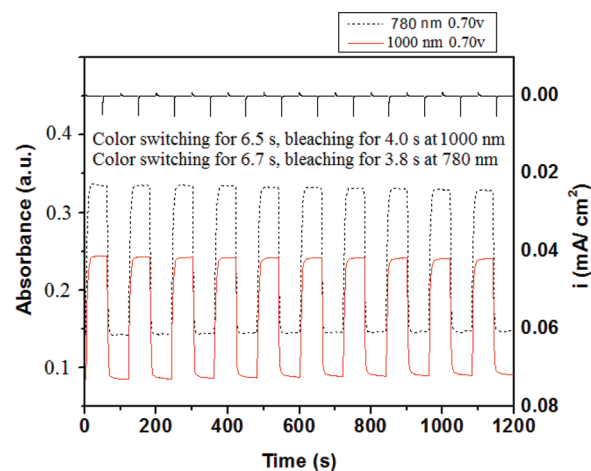


**Figure 5.** Current consumption and potential step absorptometry of poly(HNBPYTPAM) in  $\text{CH}_3\text{CN}$  with 0.1 M TBAP as the supporting electrolyte by applying a potential step (0.00–0.70 V).

not shifted, indicating that the polymer is stable to redox. The redox potentials should be shifted if the electropolymerization occurred.<sup>31</sup> Therefore, the fixed redox potentials means the electropolymerized did not occur in the polymer. This is because the para-positions of the triphenylamine were replaced by the 2-phenylpropyl moiety, which has been reported in our previous work.<sup>32</sup>

**2.4. Electrochromic Characteristics.** For the electrochromic investigations, poly(HNBPYTPAM) was cast on graphene-coated PET slides and ITO-coated glass slides and a homemade electrochemical cell was built from a commercial UV–visible cuvette. The sheet resistance of Graphene and ITO are 2–5  $\text{K}\Omega/\text{sq}$  and 88.34  $\Omega/\text{sq}$ , respectively. The cell was placed in the optical path of the sample light beam in a UV–vis–NIR spectrophotometer, which allowed us to acquire electronic absorption spectra in situ under potential control in a 0.1 M TBAP/ $\text{CH}_3\text{CN}$  solution. The results of PHNBPYTPAM-G film (thickness about 10  $\mu\text{m}$ ) are presented in Figure 4A as a series of UV–vis–NIR absorbance curves correlated to electrode potentials. When the applied potentials increased positively from 0 to 1.6 V, the characteristic peak of absorbance at 800 nm increased in intensity for neutral form of poly(HNBPYTPAM) and the absorbance in the NIR region at 1400 nm gradually increased in intensity. When the potential was increased to 2.5 V, the characteristic peak at 560 nm increased. Meanwhile, the peak at 800 nm decreased in intensity. Thus, the color of the electrochromic film changed from the light yellow to green and then to a blue. For PHNBPYTPAM-ITO as shown in Figure 4B, when the applied potentials increased positively from 0 to 0.70 V, the characteristic peaks of absorbance at 800 nm increased in intensity for neutral form of poly(HNBPYTPAM). When the potential was increased to 1.10 V, corresponding to the second step oxidation, the peak at 560 nm increased. PHNBPYTPAM-G film needed a little higher operation voltages than PHNBPYTPAM-ITO film to switch color changes and performed similar spectral changes with PHNBPYTPAM-ITO film. The spectral changes (color changes) depend on the structure of polymers and the switching voltages are related to electrodes. The observed UV–vis–NIR absorption changes in PHNBPYTPAM-G and PHNBPYTPAM-ITO films at various potentials are fully reversible and are associated with strong color changes.

For electrochromic switching studies, polymer films were cast on ITO-coated glass slides in the same manner as described above.

Although the films were switched, the absorbance at the given wavelength was monitored as a function of time with UV–vis–NIR spectroscopy. The switching data of poly(HNBPYTPAM) are shown in Figure 5. The switching time was calculated at 90% of the full switch because of the difficulty to perceive any further color changes with the naked eye beyond this point. Thin Poly-(HNBPYTPAM) film at 0.70 V both required 6.5 s for switching time and 4.0 s for bleaching time in the NIR region. In the UV–vis region, thin Poly(HNBPYTPAM) film at 0.70 V required 6.7 s for switching and 3.8 s for bleaching at 780 nm. Continuous cyclic scans between 0.00 and 0.70 V, the Poly(HNBDTPA) film exhibited good stability of electrochromic characteristics.

### 3. EXPERIMENTAL SECTION

**Preparation of CVD Graphene.** Large-area single-layered graphene was grown by CVD on 25 mm copper foil (Alfa Aesar). A flow of 15 sccm H<sub>2</sub> and 65 sccm CH<sub>4</sub> was introduced at graphene growth temperature of 1000 °C.<sup>33</sup> Before growth, plasma was applied to remove the oxide layer of copper. After CVD growth, a transfer process with PMMA (15k, 4.6 wt %) coating was required. Copper etchant Ferric Nitride (0.05 mg·mL<sup>-1</sup>) was used to etch away the copper foil substrate, leaving a transparent PMMA thin film floating on etchant solution. PMMA film was then washed by D.I. water and transferred onto PET substrates. The sheet resistance of the film is ~1k to 2k Ω/sq and the transparency is 97.5% (at 550 nm). The UV absorption spectrum is used to confirm the graphene layer since monolayer graphene absorb ~2.3% of visible light (say 550 nm). The UV absorption spectrum on our sample (graphene/PET) shows the transparency of 94–97%, suggesting less than three layers of graphene were formed on PET substrate.

### 4. CONCLUSIONS

In summary, a novel thermally stable polynorbornene with asymmetric electroactive moieties were designed and prepared via ring-opening metathesis polymerization. The polynorbornene showed remarkable solvatochromism, excellent electrochemical stability and reversible electrochromic behavior. Electrochromic devices made from the thermally stable polynorbornene and high transparent graphene electrode coated on PET substrate (PHNBPYTPAM-G) or ITO-coated substrate (PHNBPYTPAM-ITO) were successfully fabricated. Although the oxidation potential for its color changing is higher than that on ITO substrates, which is likely attributed to that CVD graphene possesses higher sheet resistance than ITO, the polynorbornene active layer on CVD graphene electrodes still sustains its intrinsic electrochromic properties; i.e., its color can be tuned from light yellow, to green and then blue with increasing applied voltage. The results mean flexible electrochromic devices using flexible graphene-coated substrate are feasible.

### ■ ASSOCIATED CONTENT

**Supporting Information.** Synthesis and characterization details for the monomers and polymers and cyclic voltammograms with 100 cycles. This material is available free of charge via the Internet at <http://pubs.acs.org/>.

### ■ AUTHOR INFORMATION

#### Corresponding Author

\*Telephone: 886-2-27376638 or 886-2-27335050. Fax: 886-2-23781441 or 886-2-27376644. E-mail: liawdj@mail.ntust.edu.tw, liawdj@gmail.com, liawdj@ntu.edu.tw, liawdj@yahoo.com.tw.

### ■ ACKNOWLEDGMENT

The authors would like to thank the National Science Council of the Republic of China for the financial support of this work.

### ■ REFERENCES

- (1) Scott, J. C.; Kaufman, J. H.; Brock, P. J.; DiPietro, R.; Salem, J.; Goitia, J. A. *J. Appl. Phys.* **1996**, *79*, 2745–2751.
- (2) Zhang, Y.; Tan, Y. W.; Stormer, H. L.; Kim, P. *Nature* **2005**, *438*, 201–204.
- (3) Orlita, M.; Faugeras, C.; Plochocka, P.; Neugebauer, P.; Martinez, G.; Maude, D. K.; Barra, A. L.; Sprinkle, M.; Berger, C.; De Heer, W. A.; Potemski, M. *Phys. Rev. Lett.* **2008**, *101*.
- (4) Wang, X.; Zhi, L.; Müllen, K. *Nano Lett.* **2008**, *8*, 323–327.
- (5) Geim, A. K.; Novoselov, K. S. *Nat. Mater.* **2007**, *6*, 183–191.
- (6) Lee, C.; Wei, X.; Kysar, J. W.; Hone, J. *Science* **2008**, *321*, 385–388.
- (7) Liu, Z.; Liu, Q.; Huang, Y.; Ma, Y.; Yin, S.; Zhang, X.; Sun, W.; Chen, Y. *Adv. Mater.* **2008**, *20*, 3924–3930.
- (8) Novoselov, K. S.; Geim, A. K.; Morozov, S. V.; Jiang, D.; Zhang, Y.; Dubonos, S. V.; Grigorieva, I. V.; Firsov, A. A. *Science* **2004**, *306*, 666–669.
- (9) Hernandez, Y.; Nicolosi, V.; Lotya, M.; Blighe, F. M.; Sun, Z.; De, S.; McGovern, I. T.; Holland, B.; Byrne, M.; Gun'ko, Y. K.; Boland, J. J.; Niraj, P.; Duesberg, G.; Krishnamurthy, S.; Goodhue, R.; Hutchison, J.; Scardaci, V.; Ferrari, A. C.; Coleman, J. N. *Nat. Nanotechnol.* **2008**, *3*, 563–568.
- (10) Dikin, D. A.; Stankovich, S.; Zimney, E. J.; Piner, R. D.; Dommett, G. H. B.; Evmenenko, G.; Nguyen, S. T.; Ruoff, R. S. *Nature* **2007**, *448*, 457–460.
- (11) Eda, G.; Fanchini, G.; Chhowalla, M. *Nat. Nanotechnol.* **2008**, *3*, 270–274.
- (12) Li, D.; Müller, M. B.; Gilje, S.; Kaner, R. B.; Wallace, G. G. *Nat. Nanotechnol.* **2008**, *3*, 101–105.
- (13) Ohta, T.; Bostwick, A.; Seyller, T.; Horn, K.; Rotenberg, E. *Science* **2006**, *313*, 951–954.
- (14) Berger, C.; Song, Z.; Li, X.; Wu, X.; Brown, N.; Naud, C.; Mayou, D.; Li, T.; Hass, J.; Marchenkov, A. N.; Conrad, E. H.; First, P. N.; De Heer, W. A. *Science* **2006**, *312*, 1191–1196.
- (15) Su, C. Y.; Lu, A. Y.; Xu, Y.; Chen, F. R.; Khlobystov, A. N.; Li, L. J. *ACS Nano* **2011**, *5*, 2332–2339.
- (16) Kim, K. S.; Zhao, Y.; Jang, H.; Lee, S. Y.; Kim, J. M.; Ahn, J. H.; Kim, P.; Choi, J. Y.; Hong, B. H. *Nature* **2009**, *457*, 706–710.
- (17) Eda, G.; Lin, Y. Y.; Miller, S.; Chen, C. W.; Su, W. F.; Chhowalla, M. *Appl. Phys. Lett.* **2008**, *92*, 233305.
- (18) Hong, W.; Xu, Y.; Lu, G.; Li, C.; Shi, G. *Electrochem. Commun.* **2008**, *10*, 1555–1558.
- (19) Wu, J.; Becerril, H. A.; Bao, Z.; Liu, Z.; Chen, Y.; Peumans, P. *Appl. Phys. Lett.* **2008**, *92*, 263302.
- (20) Wang, X.; Zhi, L.; Tsao, N.; Tomović, Ž.; Li, J.; Müllen, K. *Angew. Chem., Int. Ed.* **2008**, *47*, 2990–2992.
- (21) Chen, W. H.; Wang, K. L.; Liaw, D. J.; Lee, K. R.; Lai, J. Y. *Macromolecules* **2010**, *43*, 2236–2243.
- (22) Chen, W. H.; Wang, K. L.; Hung, W. Y.; Jiang, J. C.; Liaw, D. J.; Lee, K. R.; Lai, J. Y.; Chen, C. L. *J. Polym. Sci., Part A: Polym. Chem.* **2010**, *48*, 4654–4667.
- (23) Chang, C. H.; Wang, K. L.; Jiang, J. C.; Liaw, D. J.; Lee, K. R.; Lai, J. Y.; Lai, K. H. *Polymer* **2010**, *51*, 4493–4502.
- (24) Chang, C. H.; Wang, K. L.; Jiang, J. C.; Liaw, D. J.; Lee, K. R.; Lai, J. Y.; Chiu, K. Y.; Su, Y. O. *J. Polym. Sci., Part A: Polym. Chem.* **2010**, *48*, 5659–5669.
- (25) Wu, H. Y. U.; Wang, K. L. I.; Jiang, J. C.; Liaw, D. J.; Lee, K. R.; Lai, J. Y.; Chen, C. L. *J. Polym. Sci., Part A: Polym. Chem.* **2010**, *48*, 3913–3923.
- (26) Wu, H. Y.; Wang, K. L.; Liaw, D. J.; Lee, K. R.; Lai, J. Y. *J. Polym. Sci., Part A: Polym. Chem.* **2010**, *48*, 1469–1476.
- (27) Liaw, D. J.; Chang, F. C.; Leung, M. K.; Chou, M. Y.; Muellen, K. *Macromolecules* **2005**, *38*, 4024–4029.

- (28) Delaude, L.; Demonceau, A.; Noels, A. F. *Macromolecules* **1999**, *32*, 2091–2103.
- (29) Reichardt, C. *Chem. Rev.* **1994**, *94*, 2319–2358.
- (30) Liaw, D. J.; Wang, K. L. I.; Lee, K. R.; Lai, J. Y. *J. Polym. Sci., Part A: Polym. Chem.* **2007**, *45*, 3022–3031.
- (31) Seo, E. T.; Nelson, R. F.; Fritsch, J. M.; Marcoux, L. S.; Leedy, D. W.; Adams, R. N. *J. Am. Chem. Soc.* **1966**, *88*, 3498–3503.
- (32) Wu, H. Y.; Wang, K. L.; Jiang, J. C.; Liaw, D. J.; Lee, K. R.; LAI, J. Y.; Chen, C. L. *J. Polym. Sci., Part A: Polym. Chem.* **2010**, *48*, 3913–3923.
- (33) Li, X.; Cai, W.; An, J.; Kim, S.; Nah, J.; Yang, D.; Piner, R.; Velamakanni, A.; Jung, I.; Tutuc, E.; Banerjee, S. K.; Colombo, L.; Ruoff, R. S. *Science* **2009**, *324*, 1312–1314.